



# Experimental Investigation of Polymeric Beam Under Elastic and Plastic Loads

Mohammed Dukhi Almutairi\*

School of Aerospace, Transport, and Manufacturing, Cranfield University, Cranfield, UK

Muhammad A Khan

School of Aerospace, Transport, and Manufacturing, Cranfield University, Cranfield, UK

**Abstract:** Three-dimensional (3D) printing is now one of the most essential industrial production technologies. However, the most commonly used material in Fused Deposition Modelling (FDM) technology is Acrylonitrile Butadiene Styrene (ABS), has excellent mechanical properties. During the last few decades, researchers have focused on issues related to self-healing materials. However, because of their low mechanical strength, self-healing materials have yet to find widespread application. In this work, the behaviour of polymeric beams made of TPU “roller” materials and their responses under load is developed. One type of 3D-printed beam was designed to test different force ranges (0–0.73575 N) and deflection resolutions (15 mm–19 mm) with respect to the length. An assessment was also made of the self-healing mechanism, which encompasses the intrinsic and extrinsic techniques for each application. In terms of an extrinsic procedure, external healing agents such as micro-capsules were introduced into the system. But we came up with a way to estimate the length of the crack tip based on the relationship between the force applied and the load frame’s movement. Origami capsule-based healing systems are a well-known technology that has multiple uses in smart materials.

**Keywords:** 3D printing, crack propagation, origami capsule TPU, self-healing mechanism, DCB

**Received:** 12 February 2022; **Accepted:** 23 May 2022; **Published:** 15 August 2022

## I. INTRODUCTION

A field expanding rapidly nowadays is Three-dimensional (3D) printing or the Additive Manufacturing (AM) of smart polymers. The variety of AM techniques available suggests it may be possible to manufacture costly but smart materials flexibly with minimum waste. The on-demand or autonomous repair of different forms of damage such as cracks or scratches can increase the operational life of products and is facilitated through the use of artificial polymers such as autogenous or intrinsic self-healing.

Materials and structural components are characterized by their ability to break or fracture due to external force. This force can be mechanical, thermal or chemical, causing radiation or a combination of these factors [1]. According to this study, life efficiency and overall

strength reduce when a structure is damaged or broken [2]. However, the type of damage also plays a significant role in adapting the repair mode for a particular structure, which often makes the overall process complex and time-consuming [3]. Origami based structures can be used with the laminated composites to make light-weight structures that are capable of reducing the effect of crack propagation. Usually, OSH is applied to the areas where crack propagation has made great changes in the surface area [4]. An alternative avenue to pursue in creating smart 3D printed products is to embed novel origami-inspired capsules in the layers of a printed component. For essential applications, in particular, such capsules could create an artificial hormone network that will make 3D printed products safer and considerably more dependable [5, 6, 7]. A cost-effective solution for production on a larger scale

\*Correspondence concerning this article should be addressed to Mohammed Dukhi Almutairi, School of Aerospace, Transport, and Manufacturing, Cranfield University, Cranfield, UK. E-mail: [m.almutairi@cranfield.ac.uk](mailto:m.almutairi@cranfield.ac.uk)

is to use standard FDM to embed these capsules when printing the required component. Just as the human hormone system actuates when a virus or bacteria enters the body, a strain removal-based actuation for origami-inspired capsules can radically transform the self-healing capacity in components or structures. Strain removal of an entire component is thus initiated by surface or sub-surface damage. When strain removal occurs below the surface, the capsules begin to unfold and expand [8].

Previous research has measured the strain release in the beam using a strain gauge and microcontroller [9]. Various experiments have also been conducted to measure strain using an electrical [10, 11], optical [12] or mechanical strain gauge [13]. The strain gauge was calibrated in a windmill structure [14]. Another experiment to measure strain was performed on a cantilever beam with a sensor. The vital factor in the structure was the applied force, and Taguchi-based optimization was used to determine the optimal parameters [15]. Systems for measuring strain and its impact have also been explored by using a resistance strain gauge [16]. The promising combination of readily available healing conditions (e.g., room temperature) and the useful mechanical properties of Thermoplastic Polyurethanes (TPU) has drawn a substantial amount of scholarly interest in TPU in the wider domain of self-healing polymers. While various reversible chemistries can facilitate healing, hydrogen bonding between urethane units at the broken interface is usually the most efficient way to engender interfacial healing [6]. However, the high reversible bond density can cause microcrystals to form and inhibit macromolecular dynamics, which impedes healing.

Encapsulation based on origami has shown encouraging results [17], especially when evaluated for mechanical strength and healing capabilities on delicate and fragile materials [18]. Encapsulating folded materials, such as origami, inside stiff and static structures might produce self-healing characteristics within the structure. This helps the structure withstand harsh fatigue conditions, microcrack failure, and material deterioration [19, 20]. It also makes the material safe and durable for use, saving time, cost, and minimising inefficiency caused by damage [21].

The current study aims to investigate the elastic and plastic regimes under different bending loads.

## II. METHODOLOGY

In this paper, several techniques were used to prepare and characterize the samples. Specifically, bending load and delamination of a double cantilever beam were tested to learn more about the elastic and plastic behaviour of

the beam.

### A. Material Selection

The selected material was TPU for origami capsule. This is intriguing due to its adaptability in terms of a broad range of mechanical characteristics, excellent abrasion resistance, and low density. TPU is more elastic than ABS, making it well suited for folding into capsules. Compared to other polymers, TPU offers extra advantages, such as being exceptionally flexible, robust, and tactilely pleasant.

Beam-based, origami capsule and embedded structural beam were printed on a Raise3D Pro printer. Two printing parameters were used to create the 3D printed samples and capsule: orientation and layer thickness. The printing parameters was constant for all capsules in Table 1.

TABLE 1  
PRINTING PARAMETERS

Parameters	Value
Nozzle size (mm)	0.4
Layer thickness (mm)	0.1, 0.2
Build orientation	0°, ±45°, 90°
Infill density (%)	100

### B. Specimen Preparation

The specimen was designed as origami capsule. The inserted origami capsule's design is shown in Fig. 1, which also provides its dimensions.

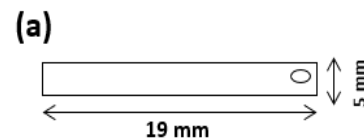


Fig. 1. Geometry of specimens: (a) origami capsule TPU "roller"

**Design of Experiment** This experimental investigation included bending load and delamination tests. Both sets of studies started with the printing of materials, including origami capsules and origami capsules embedded in beams. Using an Instron 5944 Universal Testing Machine, the specimens were next subjected to bending load and delamination tests (UTM). In particular, the bending load was applied to get a better understanding of the elastic and plastic properties of TPU.

1) *Origami beam shaped:* In this paper, the parameters were set as shown in Table 2, design of experiment methodology. The deflection data and deformation load were recorded, and the data (about strain, applied load

and deflection) were plotted using excel.

TABLE 2  
ORIGAMI CAPSULE DESIGNS

Origami Capsule Shape	Thickness (mm)	Dimensions (mm)	Loads (g)
Roller	1.0, 2.0, 3.0	19L/5W	1,2,4,6, 11,16,26

### C. Experimental Procedure

In this experiment, the end of a beam was deflected with the use of a micrometre. Before beginning the experiment, the inventor programme was used to measure the size of our basic beam and origami beam.

1) *Origami capsule behaviour*: The origami capsule insert “roller” (see Table 2). The loads were applied to the origami capsule and measurements take via computer using the signal express unit and data logger. The experiment was conducted using three tubes with different thicknesses of 1, 2, and 3 mm. The related strain readings were recorded each time the camera was set to a specified setting. Take the average after repeating the tests. Fig. 2 show the origami shape, which was designed by using inventor software, the design of capsule was confined under the initial pre-stressed condition.

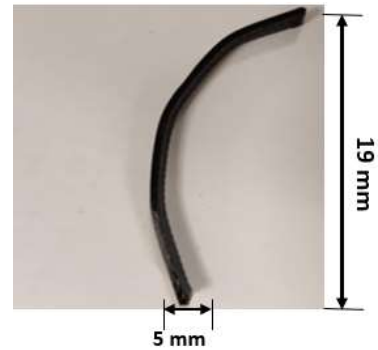


Fig. 2. Origami capsule "roller"

### III. RESULTS

This section describes the displacement response of the TPU “roller” material with different thickness values and bending loads applied at the tip of the capsule. The behaviour under an elastic regime for each origami capsule and a plastic regime for each model is shown in Table 3. Initial examination of the findings reveals that the deflection of the results varies, yielding a maximum deflection of 19 mm for the 1 mm thick capsule, within elastic limits. However, for the 2 mm thick capsule, a deflection of 17 mm was observed. For a 3 mm thick capsule, the maximum stress yielded a deflection of 15 mm. Table 3 also represents the green values, which is a primary indication of initiation of the plastic regime of each capsule at different beam thicknesses.

TABLE 3  
DATA COLLECTED FOR FORCE AND MAXIMUM DEFLECTION FOR THE TPU ORIGAMI CAPSULE "ROLLER"

1 mm		2 mm		3 mm	
Force (N)	Max Deflection (mm)	Force (N)	Max Deflection (mm)	Force (N)	Max Deflection (mm)
0	0	0	0	0	0
0.00981	2	0.00981	2	0.00981	2
0.01962	4	0.01962	4	0.01962	4
0.03924	7	0.03924	7	0.03924	5
0.05886	9	0.05886	10	0.05886	7
0.10791	13	0.10791	12	0.10791	9
0.15696	17	0.15696	15	0.15696	11
0.25506	19	0.25506	17	0.25506	13
		0.35316	19	0.35316	15
				0.54936	17
				0.73575	19

Given the observed changes for the maximum deflection with respect to different loads, it is helpful to analyse whether the values change with position or not. This was done by plotting a 3D-surface graph. To clearly

understand this concept, a 3D-surface plot that shows the parametric relationship between force, deflection, and position of the capsule, was used to observe the results (see Fig. 3).

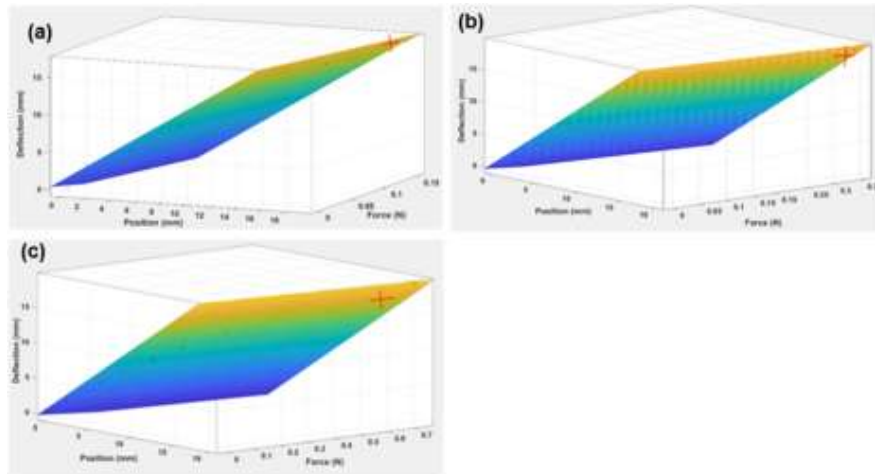


Fig. 3. 3D gradient graph of the TPU capsule "roller" plotted between Force (N), Deflection (mm) and Position (mm) at thicknesses of (a) 1mm, (b) 2mm, and (c) 3mm

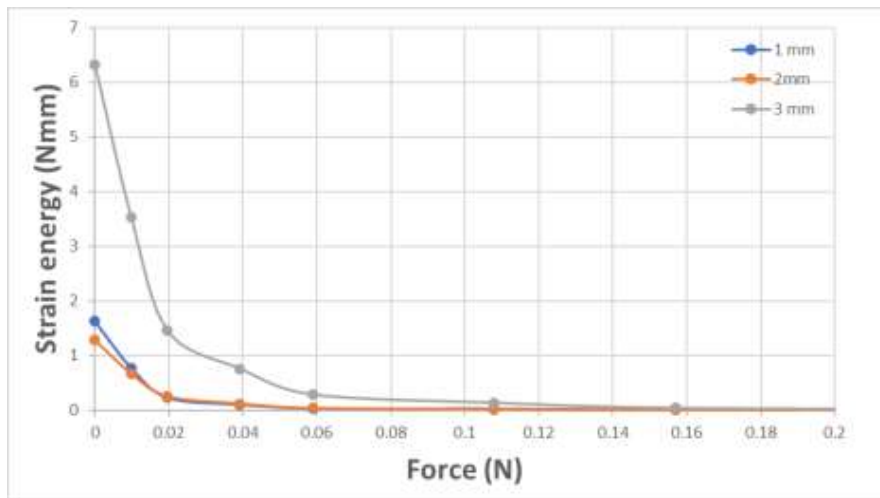


Fig. 4. Strain energy versus applied force for the TPU “roller” capsule for thicknesses of a) 1.0 mm, b) 2.0 mm, and c) 3.0 mm

Fig. 4 indicates the response of strain energy with force applied to the TPU “roller” capsule. It is clear from the trends that the responsiveness of the origami capsule to strain energy is exponential and, for all capsule thicknesses, diminishes as the applied force increases. It is evident that a force of 0.2 N is the maximum for showing the response of strain energy from all three capsule thicknesses. Deflection as a function of force and position is observed for the TPU “roller”. From the 3-D surface graphs, it is evident that a plastic region was reached at the maximum values of applied load for each thickness of the TPU “roller” origami capsule.

Mathematically expressed,  
 deflection =  $f(\text{force, position})$

For the TPU “roller”, the generalized equation for any arbitrary point to Equation 1 is

$f$  deflection ( $x = \text{force, } y = \text{position at any point}$ )

$$p00 + p10x + p01y \tag{1}$$

where,  $p1, p2,$  and  $p3$  indicate the coefficients of a polynomial equation in which  $x$  is the thickness of the capsule.

The results of the coefficients at different small beams thickness are summarised in Table 4.

TABLE 4  
 DIFFERENT VALUES OF COEFFICIENTS OF TPU  
 "ROLLER" CAPSULES OF DIFFERENT THICKNESSES

Thickness	P00	P10	P01	R-squared
1 mm	1.20	-23.57	1.05	0.9865
2 mm	0.58	-8.39	1.12	0.9977
3 mm	0.67	-3.10	1.07	0.9970

By substituting the coefficients in Equation 1, the polynomial equation for each thickness of the roller capsule can easily be found.

$$1.0mm f(x,y) = 1.20 - 23.57x + 1.05y \tag{2}$$

$$2.0mm f(x,y) = 0.58x - 8.39x + 1.12y \quad (3)$$

$$3.0mm f(x,y) = 0.67 - 3.10x + 1.07y \quad (4)$$

As Table 4 above shows, the  $R$ -squared values for each thickness were found to be 0.9865, 0.9977 and 0.9970, respectively for the 1 mm, 2 mm, and 3 mm “roller” capsule thickness. Therefore, the 3.0 mm thick capsule has the

lowest values of coefficients and highest  $R$ -squared values. The results can be simplified even further if the variables and coefficients are reduced by plotting the coefficient curves against beam thickness, allowing the corresponding slopes of the curves to be determined (the coefficients  $r_1$ ,  $r_2$ , and  $r_3$ ) as shown in Fig. 5.

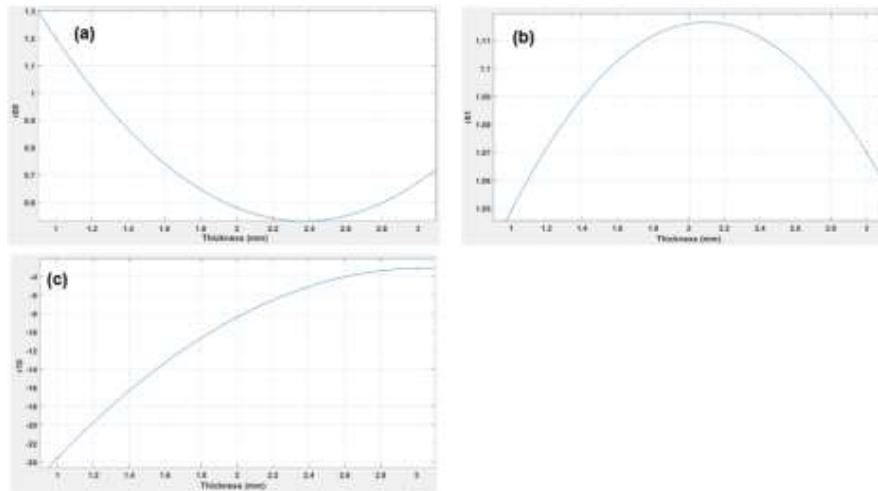


Fig. 5. Graphs indicating the relationship of TPU "roller" capsule thickness versus coefficient for (a)  $r_{00}$ , (b)  $r_{01}$  and (c)  $r_{10}$

Each graph in Fig. 5 was fitted with a second-degree polynomial, so the simplified equation becomes:

$$f(x = thickness) = r_1x^2 + r_2x + r_3 \quad (5)$$

TABLE 5  
VALUES OF LINEAR EQUATION COEFFICIENTS FOR ALL THREE THICKNESS OF TPU "ROLLER" CAPSULE

Coefficient	$r_1$	$r_2$	$r_3$	$R$ -squared
$r_{00}$	0.357	-10.692	2.536	1.00
$r_{01}$	-0.0565	0.2365	0.869	1.00
$r_{10}$	-4.943	30.01	-48.63	1.00

The generalised equation is obtained by substituting the values of the coefficients in Equation 5:

$$r_{00}f(x) = 0.357x^2 - 10.692x + 2.536 \quad (6)$$

$$r_{01}f(x) = -0.0565x^2 + 0.2365x + 0.869 \quad (7)$$

$$r_{10}f(x) = -4.943x^2 + 30.01x - 48.63 \quad (8)$$

The above equations are formulated by substituting the values in the generalised equation. The  $R$ -squared value for each coefficient is 1.00, which shows a perfect fit of curve, as indicated in Table 5.

#### IV. DISCUSSION

The current analysis is predicated on the observation that elastic and plastic strains are not independent and that the influence of transformation plasticity may be included in a general phenomenological analysis that conforms to the formalism of macroscale elasticity theory. Fig. 3 depicts the experimentally obtained mean load, deflection, and position of the bending tests for each thickness of roller, in this case 1.0 mm, 2.0 mm, and 3.0 mm. The plastic region was attained at the maximum values of applied load for each thickness of the TPU “roller” capsule, according to the analysis of 3D curves as shown in Fig. 3. The  $R$ -squared value for the thickness values was 0.9865, 0.9977, and 0.9970 respectively for the 1.0 mm, 2.0 mm, and 3.0 mm capsules. As shown in Table 4, as the TPU “roller” capsule thickness increases, the accuracy of the model equation decreases. This demonstrates that the equation is less suitable for thicker beams. The maximum stress values for 1.0 mm, 2.0 mm, and 3.0 mm capsules were  $0.22 \times 10$  Pa,  $0.73 \times 10$  Pa, and  $0.90 \times 10$  Pa, respectively.

Table 3 shows the recorded values for the TPU “roller” capsule. The elastic limit of the beam was observed to be about 0.26 N for the 1.0 mm thick beam, 0.26 N for 2mm, and 0.35 N for 3mm after the green values, which is a primary indication of the initiation of the plastic region of the capsule at different thicknesses.

Fig. 4 shows that the strain energy for all three capsules is obtained at a maximum of 0.2 N. However, the overall strain energy decay was significantly affected by the capsule thickness. Because the material is more resilient, the TPU “roller” capsules may be ideal for higher stresses. In Fig. 5  $r_{00}$ ,  $r_{01}$ , and  $r_{10}$  are plotted against thickness using the model equation and corresponding to the  $R$ -squared values of 1.0 for all coefficients. In conclusion, the elastic modulus of the TPU “roller” capsule was lower than that of the TPU “cross” capsule, according to the experimental results. However, one notable effect for the TPU “roller” capsule was that the plastic region of the capsule was activated at relatively low values of applied load. This also suggests that the TPU “roller” has a high degree of flexibility, which can be used to advantage in designs where the beam must be folded and activated in response to even minor changes in applied load. The TPU “roller” is more likely to remain elastic under deformation. To check this, inserted a TPU “roller” capsule in the DCB and calculated the strain energy released by crack growth in the DCB to see what would activate the TPU “roller”. Because the strain values were calculated above, it was simple to represent the amount of strain energy released during crack propagation. The question is whether the quantity of strain energy released is sufficient to activate the TPU “roller” module.

## V. CONCLUSION

This research studied the strain energy behaviour of self-healing mechanisms under elastic and plastic conditions for TPU capsules. First, the equations corresponding to the general case of TPU “roller” capsule researchers were obtained. Origami capsules were made in the shape of a roller, folded or elastically deformed and embedded in the main beam structure. Different capsule thicknesses were tested for elastic-plastic load, deflection, and position. The elastic study of the stress and strain energy concentration from the origami capsule’s roller form showed that the largest stress concentration occurs at the capsule’s tipoff and in the load application area. The results demonstrate the potential of origami capsules as a unique self-healing mechanism to augment current practise, which is mostly dependent on external healing agents. Future work will examine how strain release to the embedded structure works.

## REFERENCES

- [1] C. Bucknall, I. Drinkwater, and G. Smith, “Hot plate welding of plastics: Factors affecting weld strength,” *Polymer Engineering & Science*, vol. 20, no. 6, pp. 432–440, 1980. doi: <https://doi.org/10.1002/pen.760200609>
- [2] D. Liu, C. Lee, and X. Lu, “Repairability of impact-induced damage in SMC composites,” *Journal of Composite Materials*, vol. 27, no. 13, pp. 1257–1271, 1993. doi: <https://doi.org/10.1177/002199839302701302>
- [3] T. Osswald and G. Menges, “Failure and damage of polymers,” in *Materials science of polymers for engineers*. Munich, Germany: Hanser Publishers, 2003, p. 447.
- [4] V. S. C. Chillara, L. M. Headings, and M. J. Dapino, “Self-folding laminated composites for smart origami structures,” in *Smart Materials, Adaptive Structures and Intelligent Systems*, Colorado, CO, 2015. doi: <https://doi.org/10.1115/SMASIS2015-8968>
- [5] M. E. Belowich and J. F. Stoddart, “Dynamic imine chemistry,” *Chemical Society Reviews*, vol. 41, no. 6, pp. 2003–2024, 2012. doi: <https://doi.org/10.1039/C2CS15305J>
- [6] B. Willocq, J. Odent, P. Dubois, and J.-M. Raquez, “Advances in intrinsic self-healing polyurethanes and related composites,” *RSC Advances*, vol. 10, no. 23, pp. 13 766–13 782, 2020. doi: <https://doi.org/10.1039/D0RA01394C>
- [7] Z. P. Zhang, M. Z. Rong, and M. Q. Zhang, “Mechanically robust, self-healable, and highly stretchable “living” crosslinked polyurethane based on a reversible C-C bond,” *Advanced Functional Materials*, vol. 28, no. 11, p. 1706050, 2018. doi: <https://doi.org/10.1002/adfm.201706050>
- [8] M. D. Almutairi, A. I. Aria, V. K. Thakur, and M. A. Khan, “Self-healing mechanisms for 3D-printed polymeric structures: From lab to reality,” *Polymers*, vol. 12, no. 7, pp. 1–27, 2020. doi: <https://doi.org/10.3390/polym12071534>
- [9] J. C. Butler, A. J. Vigliotti, F. W. Verdi, and S. M. Walsh, “Wireless, passive, resonant-circuit, inductively coupled, inductive strain sensor,” *Sensors and Actuators A: Physical*, vol. 102, no. 1-2, pp. 61–66, 2002. doi: [https://doi.org/10.1016/S0924-4247\(02\)00342-4](https://doi.org/10.1016/S0924-4247(02)00342-4)
- [10] D. J. Cohen, D. Mitra, K. Peterson, and M. M. Ma-harbiz, “A highly elastic, capacitive strain gauge based on percolating nanotube networks,” *Nano Letters*, vol. 12, no. 4, pp. 1821–1825, 2012. doi: <https://doi.org/10.1021/nl204052z>
- [11] L. Laloui, M. Nuth, and L. Vulliet, “Experimental and numerical investigations of the behaviour of a heat exchanger pile,” *International Journal for Numerical and Analytical Methods in Geome-*

- chanics, vol. 30, no. 8, pp. 763–781, 2006. doi: <https://doi.org/10.1002/nag.499>
- [12] K. Lim, C. Chew, P. Chen, S. Jeyapalina, H. Ho, J. Rappel, and B. Lim, “New extensometer to measure in vivo uniaxial mechanical properties of human skin,” *Journal of Biomechanics*, vol. 41, no. 5, pp. 931–936, 2008.
- [13] J. Hale and M. Chapman, “Design, installation and calibration of a strain gauge structural monitoring system for a timber windmill,” *Experimental Techniques*, vol. 38, no. 3, pp. 45–53, 2014. doi: <https://doi.org/10.1111/j.1747-1567.2011.00801.x>
- [14] M. Moayyedean, J. F. Derakhshandeh, and S. H. Lee, “Optimization of strain measurement procedure based on fuzzy quality evaluation and taguchi experimental design,” *SN Applied Sciences*, vol. 1, no. 11, pp. 1–11, 2019. doi: <https://doi.org/10.1007/s42452-019-1428-x>
- [15] A. Kumar, S. K. Chaturvedi, V. Chaturvedi, and R. C. Yadaw, “Design studies and optimization of position of strain gauge,” *International Journal of Scientific & Engineering Research*, vol. 3, no. 10, pp. 1–4, 2012.
- [16] Y. Yamagata, X. Lu, Y. Sekiguchi, and C. Sato, “Experimental investigation of mode I fracture energy of adhesively bonded joints under impact loading conditions,” *Applied Adhesion Science*, vol. 5, no. 1, pp. 1–10, 2017. doi: <https://doi.org/10.1186/s40563-017-0087-7>
- [17] J. K. Banshiwal and D. N. Tripathi, “Self-healing polymer composites for structural application,” in *Functional Materials*. London, UK: IntechOpen, 2019.
- [18] G. Yıldırım, A. H. Khiavi, S. Yeşilmen, and M. Şahmaran, “Self-healing performance of aged cementitious composites,” *Cement and Concrete Composites*, vol. 87, pp. 172–186, 2018. doi: <https://doi.org/10.1016/j.cemconcomp.2018.01.004>
- [19] M. Alazhari, T. Sharma, A. Heath, R. Cooper, and K. Paine, “Application of expanded perlite encapsulated bacteria and growth media for self-healing concrete,” *Construction and Building Materials*, vol. 160, pp. 610–619, 2018. doi: <https://doi.org/10.1016/j.conbuildmat.2017.11.086>
- [20] O. Teall, M. Pilegis, R. Davies, J. Sweeney, T. Jefferson, R. Lark, and D. Gardner, “A shape memory polymer concrete crack closure system activated by electrical current,” *Smart Materials and Structures*, vol. 27, no. 7, pp. 1–12, 2018. doi: <https://doi.org/10.1088/1361-665X/aac28a>
- [21] J. W. Pang and I. P. Bond, “A hollow fibre reinforced polymer composite encompassing self-healing and enhanced damage visibility,” *Composites Science and Technology*, vol. 65, no. 11-12, pp. 1791–1799, 2005. doi: <https://doi.org/10.1016/j.compscitech.2005.03.008>